

# Discovery of the ammonium substrate site on glutamine synthetase, a third cation binding site



SHWU-HUEY LIAW,<sup>1</sup> ICHUN KUO,<sup>1</sup> AND DAVID EISENBERG<sup>2</sup>

<sup>1</sup> Institute of Molecular Medicine, School of Medicine, National Taiwan University, Taipei, Taiwan

<sup>2</sup> UCLA–DOE Laboratory of Structural Biology and Molecular Medicine, Molecular Biology Institute and Department of Chemistry and Biochemistry, University of California, Los Angeles, California 90095-1570

(RECEIVED April 11, 1995; ACCEPTED August 30, 1995)

## Abstract

Glutamine synthetase (GS) catalyzes the ATP-dependent condensation of ammonia and glutamate to yield glutamine, ADP, and inorganic phosphate in the presence of divalent cations. Bacterial GS is an enzyme of 12 identical subunits, arranged in two rings of 6, with the active site between each pair of subunits in a ring. In earlier work, we have reported the locations within the funnel-shaped active site of the substrates glutamate and ATP and of the two divalent cations, but the site for ammonia (or ammonium) has remained elusive. Here we report the discovery by X-ray crystallography of a binding site on GS for monovalent cations, Tl<sup>+</sup> and Cs<sup>+</sup>, which is probably the binding site for the substrate ammonium ion. Fourier difference maps show the following. (1) Tl<sup>+</sup> and Cs<sup>+</sup> bind at essentially the same site, with ligands being Glu 212, Tyr 179, Asp 50', Ser 53' of the adjacent subunit, and the substrate glutamate. From its position adjacent to the substrate glutamate and the cofactor ADP, we propose that this monovalent cation site is the substrate ammonium ion binding site. This proposal is supported by enzyme kinetics. Our kinetic measurements show that Tl<sup>+</sup>, Cs<sup>+</sup>, and NH<sub>4</sub><sup>+</sup> are competitive inhibitors to NH<sub>2</sub>OH in the  $\gamma$ -glutamyl transfer reaction. (2) GS is a trimetallic enzyme containing two divalent cation sites ( $n_1$ ,  $n_2$ ) and one monovalent cation site per subunit. These three closely spaced ions are all at the active site: the distance between  $n_1$  and  $n_2$  is 6 Å, between  $n_1$  and Tl<sup>+</sup> is 4 Å, and between  $n_2$  and Tl<sup>+</sup> is 7 Å. Glu 212 and the substrate glutamate are bridging ligands for the  $n_1$  ion and Tl<sup>+</sup>. (3) The presence of a monovalent cation in this site may enhance the structural stability of GS, because of its effect of balancing the negative charges of the substrate glutamate and its ligands and because of strengthening the "side-to-side" intersubunit interaction through the cation–protein bonding. (4) The presence of the cofactor ADP increases the Tl<sup>+</sup> binding to GS because ADP binding induces movement of Asp 50' toward this monovalent cation site, essentially forming the site. This observation supports a two-step mechanism with ordered substrate binding: ATP first binds to GS, then Glu binds and attacks ATP to form  $\gamma$ -glutamyl phosphate and ADP, which complete the ammonium binding site. The third substrate, an ammonium ion, then binds to GS, and then loses a proton to form the more active species ammonia, which attacks the  $\gamma$ -glutamyl phosphate to yield Gln. (5) Because the products (Glu or Gln) of the reactions catalyzed by GS are determined by the molecule (water or ammonium) attacking the intermediate  $\gamma$ -glutamyl phosphate, this negatively charged ammonium binding pocket has been designed naturally for high affinity of ammonium to GS, permitting glutamine synthesis to proceed in aqueous solution.

**Keywords:** glutamine synthetase; NH<sub>4</sub><sup>+</sup>; Tl<sup>+</sup>

Glutamine synthetase (GS) is a primary biological catalyst in the sense that it catalyzes the first step at which nitrogen is brought into cellular metabolism: glutamate + NH<sub>4</sub><sup>+</sup> + ATP → glutamine + ADP + Pi. The product glutamine is a source of nitrogen in the biosynthesis of many other metabolites (Stadtman, 1973). The reactant ammonia, released by nitrate reduction,

amino acid degradation, and photorespiration, is toxic and must be removed. In most plants, the glutamine synthetase/glutamate synthase pathway is the only efficient way to detoxify the ammonia (Mifflin & Lea, 1980). In animals, GS is found predominantly in brain, kidney, and liver. Moreover, GS is of special importance in the vertebrate nervous system; it is a key enzyme in the "small glutamate compartment" and is involved in the recycling of amino acid neurotransmitter molecules, such as glutamate and  $\gamma$ -aminobutyrate, released by physiologically active neurons (Hamberge et al., 1979). In short, in addition to gluta-

Reprint requests to: David Eisenberg, Department of Chemistry, Box 951970, University of California, Los Angeles, California 90024-1970; e-mail: david@ewald.mbi.ucla.edu.

mine biosynthesis, GS also provides a mechanism for ammonia assimilation and detoxification and a mechanism for termination of neurotransmitter signals (Cooper & Plum, 1987; Derouiche & Frotscher, 1991).

A 3.5-Å atomic model for 5,616 amino acid residues of dodecameric unadenylylated GS from *Salmonella typhimurium* was initially determined by X-ray crystallography by Almasy et al. (1986) and refined by Yamashita et al. (1989), and 2.8-Å refined models for both *S. typhimurium* and *Escherichia coli* were determined by Liaw et al. (1993c). Bacterial GS consists of 12 identical subunits with 622 symmetry, arranged as two face-to-face benzene rings, with unusual subunit contacts. The funnel-shaped active sites are located at the subunit interfaces in the same ring. The funnel is about 30 Å wide at its top, about 10 Å wide at the bottom, and 45 Å deep, and is open at both top and bottom. About halfway down each active site is a shelf formed by the two divalent cations and their ligands. The metal ions  $Mn^{2+}$  or  $Mg^{2+}$  are required for the activity and for the structural stability of GS (Ginsburg & Stadtman, 1973; Liaw et al., 1993c). ATP binds at the top of the active site cavity and the glutamate binds at the bottom, adjacent to the  $n_1$  ion (Liaw & Eisenberg, 1994). However, the binding site of the third substrate, ammonia, has remained elusive.

The reactions catalyzed by bacterial dodecameric GS (GSI) and mammalian octameric GS (GSII) are generally the same (Stadtman & Ginsburg, 1974), and similar catalytic chemical steps in glutamine synthesis have been proposed for both GSI and GSII (Meek & Villafranca, 1980; Meister, 1980). In our earlier studies by X-ray diffraction methods, we proposed a structure-based model for the enzymatic mechanism of GS (Liaw & Eisenberg, 1994) in which we suggested that an ammonium ion rather than an ammonia initially binds to GS, then is deprotonated by Asp 50' of the adjacent subunit, forming the more active species ammonia to attack the intermediate  $\gamma$ -glutamyl phosphate to yield glutamine. This proposal is also supported by kinetic studies of Alibhai and Villafranca (1994). To provide structural support for our proposal, we have sought the ammonium ion binding site on GS. In fact, the existence of monovalent cation sites on GS was proposed because monovalent cations were found to stabilize the quaternary structure of GS (Ginsburg & Stadtman, 1973), and because alkali ions were found to compete partially with  $NH_2OH$  in the  $\gamma$ -glutamyl transfer reac-

tion (unpubl. data of P.Z. Smyrniotis & E.R. Stadtman, cited in Stadtman & Ginsburg [1974]).

The electron-dense ion  $Tl^+$  (80 electrons) has been employed to study effects of monovalent cations on protein activity (Suelter & Snell, 1977; Stellwagen & Thompson, 1979; Hill & Castellino, 1986; Takada et al., 1990) and on ion channels (Urban et al., 1980; Zeiske & van Driessche, 1983; van Driessche & Zeiske, 1985), and to probe the binding sites of monovalent cations (Urry et al., 1982; Markham, 1986; Hill et al., 1987; Gursky et al., 1992). In all these studies of effects of monovalent cations on enzymes, ion carriers, and ion channels,  $Tl^+$  has been found to bind at known  $K^+$  or  $NH_4^+$  binding sites. For example, in studies by protein crystallography, Gursky et al. (1992) found that  $Tl^+$  and  $NH_4^+$  bind to the monovalent alkali cation binding site in cubic insulin crystals. In pioneering work, Stroud et al. (1974) found that  $Tl^+$  ions on trypsin can be replaced by  $K^+$  and  $Rb^+$ . Therefore,  $Tl^+$  is used here with Fourier difference methods to define the  $NH_4^+$  binding site on GS. Also, the heavy monovalent alkali cation  $Cs^+$  (54 electrons) is used to infer whether  $Tl^+$  binds to the monovalent alkali cation site on GS.

## Results

### $Tl^+$ and $Cs^+$ binding sites

Figure 1A shows the only density peak per GS subunit in the Fourier difference map of the GS- $Tl^+$  complex, in the presence of saturated thallos acetate, at the  $3\sigma$  contour level, and Figure 1B shows the only peak in the Fourier difference map of the GS- $Cs^+$  complex, in the presence of 30 mM CsCl, at the  $1.75\sigma$  contour level. At these contour levels, there are no other significant peaks for either  $Tl^+$  or  $Cs^+$ . These difference maps show that the peaks for  $Tl^+$  and for  $Cs^+$  are superimposed, suggesting that this common binding site is the monovalent cation site (named  $M^+$ ). There is one  $M^+$  per subunit.

### Ligands for the monovalent cation

The protein ligands for the  $Tl^+$  and  $Cs^+$  ions are Glu 212, Tyr 179, Ser 53', and Asp 50' of the adjacent subunit. The  $\gamma$ -carboxylate group of the substrate glutamate, or the  $\gamma$ -imino

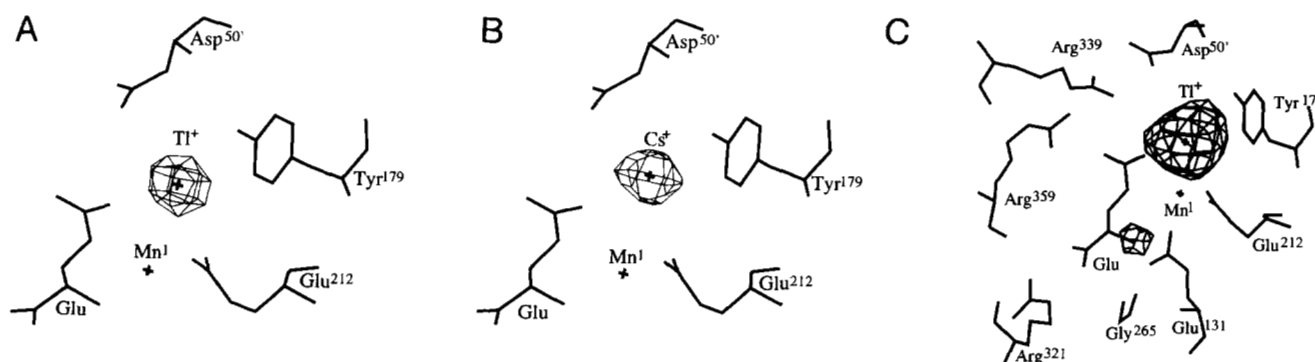


**Fig. 1.** Strongest peaks in the 12-fold averaged Fourier difference maps of GS-monovalent cation complexes. **A:** ( $F_{oGS-Tl^+} - F_{oGS}$ ), at  $3\sigma$  contour level. **B:** ( $F_{oGS-Cs^+} - F_{oGS}$ ), at  $1.75\sigma$  contour level. These density peaks show that  $Tl^+$  and  $Cs^+$  bind at the same site. **C:** ( $F_{oGS-Tl^+-NH_4^+} - F_{oGS}$ ), at  $1\sigma$  contour level. This map suggests that there may be a second weak site for  $Tl^+$  at the amino position of the substrate glutamate binding site (see Results).

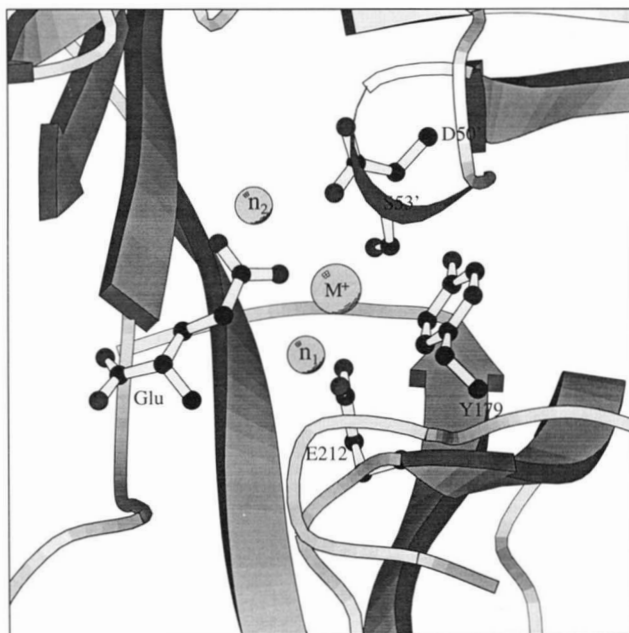


**Fig. 2.** Monovalent cation site  $M^+$  on GS drawn by the program MOLSCRIPT (Kraulis, 1991). The  $n_1$  and  $n_2$  ions are the two divalent cations. The five ligands to the  $Tl^+$  ion are shown as atomic models: substrate glutamate, Ser 53', Asp 50' (from the neighboring chain), Glu 212, and Tyr 179. Implications of this monovalent cation binding site are discussed in the text.

group of MetSox, a transition-state analogue, or the active site water molecule replaced by glutamate or MetSox (Liaw & Eisenberg, 1994) can serve as a nonprotein ligand for this monovalent cation site (Fig. 2; Kinimage 1; Table 1). These nonprotein ligands and Glu 212 also bind to the  $n_1$  ion.

#### ADP binding enhances $Tl^+$ binding to GS

In the presence of saturated thallos acetate and 1.6 mM Na·ADP, the Fourier difference map of the GS- $Tl^+$ -ADP complex shows only a single density peak appearing at the  $Tl^+$  site at the  $7\sigma$  contour level, the highest peak ever observed among our 30 GS difference maps to date, and a clear ADP peak appearing at the  $1\sigma$  contour level. Thus, the presence of ADP greatly increases  $Tl^+$  binding to GS. The reason for this enhancement is probably that ADP binding induces the movement of Asp 50' toward the  $Tl^+$  site, as has been previously observed in the GS-ADP complex (Fig. 3; Liaw & Eisenberg, 1994). Thus, the binding of ADP completes the formation of the  $Tl^+$  site.

In the presence of saturated thallos acetate and 30 mM ammonium acetate, in addition to the peak at the  $M^+$  site at the  $3\sigma$  contour level, there is a second peak at the amino position of the substrate glutamate binding site at the  $1\sigma$  contour level (Fig. 1C). The side chains of Glu 131 and Asn 265, and the carbonyl group of Gly 265, appear to be the ligands. In the complex of GS with substrate Glu (Liaw et al., 1993b), the amino group of the substrate glutamate forms hydrogen bonds with Glu 131 and Gly 265. As noted above (Fig. 1A), this second peak is not observed in the Fourier difference map of the GS- $Tl^+$  complex, perhaps due to the low solubility of thallos acetate

**Table 1.** Geometry of the monovalent cation site ( $M^+$ )<sup>a</sup>

Angle	Value (°)	Length (Å)	Value (Å)
E212OE1-M-D50'OD2	172	$n_1-n_2$	6.0
E212OE1-M-S53'OG	138	M- $n_1$	4.0
E212OE1-M-Y179OH	92	M- $n_2$	7.4
E212OE1-M-GluOE	83	M-E212OE1	2.9
E212OE2-M-D50'OD2	146	M-E212OE2	3.1
E212OE2-M-S53'OG	104	M-D50'OD2	3.3
E212OE2-M-Y179OH	103	M-S53'OG	3.3
E212OE2-M-GluOE	109	M-Y179OH	3.8
D50'OD2-M-S53'OG	46	M-GluOE	2.6
50'OD2-M-Y179OH	83		
D50'OD2-M-GluOE	95		
S53'OG-M-Y179OH	73		
S53'OG-M-GluOE	139		
Y179OH-M-GluOE	121		

<sup>a</sup> Notice that the M-ligand distances are about the 3.5 Å expected for hydrogen bonding of  $NH_4^+$  to ligands. The angles suggest slightly distorted bipyramidal bonding. The symbol Glu refers to the substrate glutamate.

(<1 mM). This site is a possible minor ammonium binding site because GS catalyzes the irreversible formation of ATP, carbon dioxide, and ammonia from carbamyl phosphate and ADP (Stadtman & Ginsburg, 1974), and because this minor site is

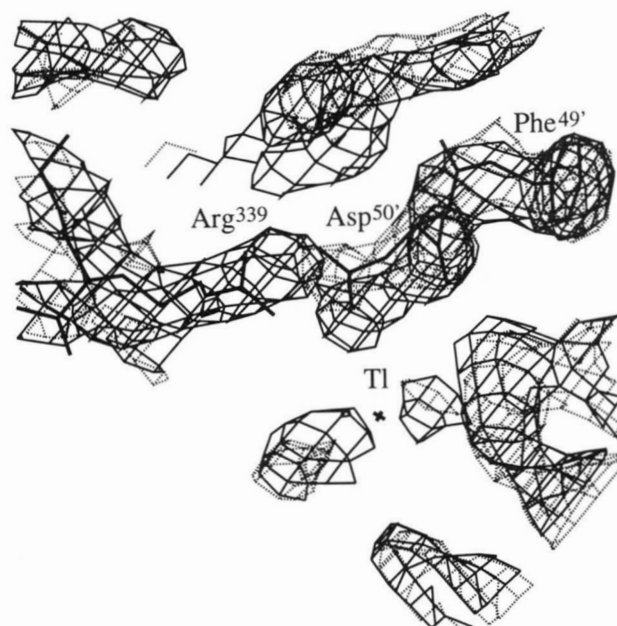


**Fig. 3.** The native GS ( $2F_o - F_c$ ) map, shown in dashed lines, and the ( $2F_o - F_c$ ) map of the GS- $Tl^+$ -ADP complex shown in solid lines. In addition to inducing the movement of Asp 50' toward the  $Tl^+$  site, ADP binding orders Arg 339: there is virtually no density observed for residue Arg 339 in GS, but the density for Arg 339 is seen in the map of the GS- $Tl^+$ -ADP complex. Thus, the ADP binding not only completes the substrate ammonium ion binding site, but also orients Arg 339 to interact with the intermediate,  $\gamma$ -glutamyl phosphate (Liaw & Eisenberg, 1994).

close to the amino position of the carbamyl phosphate binding site (S.-H. Liaw & D. Eisenberg, manuscript in prep.).

#### Kinetic measurements

To learn whether substrate ammonium ion binds at the monovalent cation site  $M^+$ , we investigated the inhibition of GS activity by monovalent alkali cations using the transferase assay. Our kinetic data suggest that  $Tl^+$ ,  $Cs^+$ , and  $NH_4^+$  are competitive inhibitors with respect to  $NH_2OH$ . Figure 4 shows a classical Lineweaver-Burke plot of  $1/\text{velocity}$  plotted as a function of  $1/[NH_2OH]$ , for  $NH_4^+$  with the indication of a common intercept on  $1/\text{velocity}$  axis, suggestive of competitive inhibition. Similar plots are observed for  $Tl^+$ ,  $Cs^+$ , and  $Li^+$ . The estimated  $K_m$  value for  $NH_2OH$  is 0.67 mM, and the  $k_i$  values for  $Tl^+$ ,  $Cs^+$ ,  $Li^+$ , and  $NH_4^+$  are 0.15, 0.51, 2.0, and 2.9 mM, respectively. Also, in single reciprocal plots ( $[NH_2OH]/\text{velocity}$  versus  $[NH_2OH]$  at various monovalent cation concentrations), parallel lines are observed with slopes of  $20 \pm 0.6$ , again suggesting competitive inhibition. Thus, kinetic studies support our structural studies that indicate that  $Tl^+$ ,  $Cs^+$ ,  $Li^+$ , and  $NH_4^+$  bind at the same site.

#### Discussion

##### $Tl^+$ binding site

The  $Tl^+$  ion binds within the funnel-shaped active site of GS, in a pocket surrounded by oxygen ligands. This pocket is reminiscent of those that bind  $Tl^+$  in trypsin (Stroud et al., 1974) and subtilisin (Drenth et al., 1972).  $Tl^+$  in GS is five- or sixfold coordinated to oxygen; it is uncertain if both oxygen atoms of the  $\gamma$ -carboxylate group of Glu 212 bind the thallos ion (Fig. 2). In contrast, the thallos ion on subtilisin is coordinated to three oxygen atoms, and the site is far removed from the catalytic center. The two thallos ions on trypsin are 2.5 Å apart; they can be replaced by  $K^+$  and  $Rb^+$ , and are three- and fivefold coordinated to oxygen. The binding of an electron-dense thallos ion at the monovalent cation site on *S. typhimurium* GS (GSI) offers the possibility of using  $Tl^+$  as a heavy-atom

derivative for the structure determination of the eukaryotic GS (GSII).

##### Does $NH_4^+$ bind at the monovalent cation site $M^+$ ?

The Fourier difference maps of GS- $Tl^+$  and GS- $Cs^+$  complexes show that  $Tl^+$  binds at an alkali monovalent cation site. We propose that an ammonium ion also binds at this site on the basis of the following. (1)  $Tl^+$  and  $NH_4^+$  are  $K^+$  analogues (Naslund & Hultin, 1981; Zeiske & van Driessche, 1983). Often these three ions bind to the same site on proteins (see Introduction). (2) The  $Tl^+$  binding site is a position from which an ammonium ion can attack the intermediate  $\gamma$ -glutamyl phosphate to yield glutamine. The distance from the  $Tl^+$  site to the putative site for the vulnerable  $\delta C$  atom of the  $\gamma$ -glutamyl phosphate is 3.4 Å. (3) Kinetic measurements suggest that  $Tl^+$ ,  $Cs^+$ , and  $NH_4^+$  compete with  $NH_2OH$  for the monovalent cation site.

##### GS is a trimetallic enzyme

There are few protein chains known that bind three metal ions. Among these are alkaline phosphatase, phospholipase C, and P1 nuclease, which have similar trimetallic (three zinc ions) constellations in the active site (Coleman, 1992). However, GS is unusual in that the active site, at the subunit interface, contains two divalent cation sites ( $n_1$ ,  $n_2$ ) and one monovalent cation site, which we term  $M^+$  (Fig. 2; Kinemage 1). The distance between  $n_1$  and  $n_2$  is 6.0 Å, between  $n_1$  and  $M^+$  is 4.0 Å, between  $n_2$  and  $M^+$  is 7.4 Å. Ions that occupy these three closely spaced ion sites are required for GS activity: the  $n_1$  metal ion is important for stabilization of the active conformation of the enzyme (Ginsburg & Stadtman, 1973; Liaw et al., 1993c); both  $n_1$  and  $n_2$  participate in the binding of the negatively charged substrates, glutamate and ATP (Liaw et al., 1993b, 1994), and in the phosphoryl transfer from ATP to glutamate (Liaw & Eisenberg, 1994) and then the glutamyl transfer from  $\gamma$ -glutamyl phosphate to ammonia. The monovalent cation site is the likely binding site of the third substrate, an ammonium ion, as explained below.

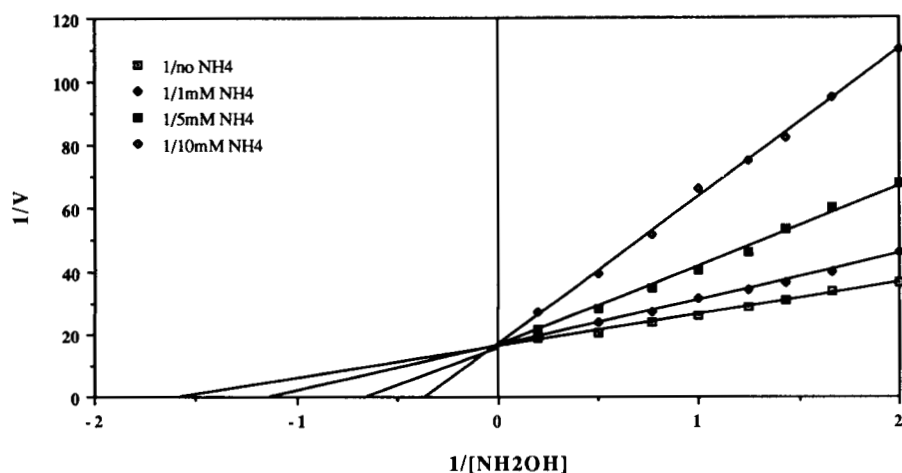


Fig. 4. Kinetic measurements by the  $\gamma$ -glutamyl transferase assay for fully unadenylylated *E. coli* GS-Mn. Double-reciprocal plot in which  $1/\text{velocity}$  is plotted as a function of  $1/[NH_2OH]$  in the presence of  $NH_4^+$ . These data suggest that  $NH_4^+$  competes with  $NH_2OH$  for its binding site.

### *Functions of the monovalent cation site on GS*

On the basis of the structures of the GS-Tl<sup>+</sup>, GS-Tl<sup>+</sup>-ADP, and GS-Cs<sup>+</sup> complexes, we propose two functions for the monovalent cation site. The first is stability. The positively charged monovalent cation contributes to the structural stability of GS. Ginsburg and Stadtman (1973) concluded that dodecameric *E. coli* GS is stabilized by Mn<sup>2+</sup> and Mg<sup>2+</sup>, and that monovalent cations stabilize of the quaternary structure of GS. Structural stabilization of GS by divalent cations, especially by the n<sub>1</sub> ion, has been ascribed to the attraction of their positive charges to the negative charges of glutamate and ATP and of their ligands (Liaw et al., 1993c). Stabilization by the monovalent cation may be due both to the electrostatic effects of its positive charge and to other components of the energy of the metal-protein bonding. Interactions of the positively charged monovalent cation with the negatively charged substrate glutamate, Glu 212, Ser 53', and Asp 50' could strengthen the active conformation. Because Ser 53' and Asp 50' reside at the subunit contact surface, the monovalent cation enhances the "side-to-side" intersubunit interaction.

The second function is to enhance the binding of the substrate ammonium ion to GS during the reaction. Ammonium binds to GS more strongly than does water, because the NH<sub>4</sub><sup>+</sup> positive charge interacts favorably in its negatively charged pocket. This is crucial to GS catalysis because the products of the reactions catalyzed by GS are determined by the molecule attacking the  $\gamma$ -glutamyl phosphate: the product is glutamine if an ammonia attacks, whereas the product is glutamate if a water molecule attacks the intermediate. Therefore, the high affinity of ammonium to GS overcomes the high concentration of water, permitting glutamine biosynthesis to proceed in aqueous solution.

### *Implications of the NH<sub>4</sub><sup>+</sup> site for the reaction mechanism*

#### *An ammonium ion is the initial substrate*

The discovery of the NH<sub>4</sub><sup>+</sup> site on GS confirms earlier conjectures (Alibhai & Villafranca, 1994; Liaw & Eisenberg, 1994) that a positively charged ammonium is the species initially binding to the negatively charged pocket on GS, before a more active ammonia, from a deprotonated ammonium, completes the reaction (Colanduoni et al., 1987).

#### *A two-step ordered substrate binding mechanism*

The observations that the presence of ADP induces movement of Asp 50' toward the NH<sub>4</sub><sup>+</sup> site, and that the  $\gamma$ -glutamyl phosphate can serve as a ligand for the NH<sub>4</sub><sup>+</sup> ion, suggest that the NH<sub>4</sub><sup>+</sup> site is fully formed after binding of both ADP and  $\gamma$ -glutamyl phosphate. Thus, identification of the NH<sub>4</sub><sup>+</sup> site supports our earlier structure-based model to explain the two-step glutamine synthesis by GS (ordered substrate binding with ATP first, then glutamate, then ammonium). The model suggests that ammonium binds to GS strongly only after the first step, in which glutamate attacks ATP to form ADP and the intermediate  $\gamma$ -glutamyl phosphate (Liaw & Eisenberg, 1994). Then, in the second step, ammonia attacks the intermediate from its nearby site, to yield glutamine.

#### *Functions of Asp 50'*

The active site of GS is located at the subunit interface and is constituted mainly by the C domain of one subunit. Most

residues involved in enzymatic catalysis are located at the C domain, but Asp 50 is contributed from the N domain of the other subunit. The function of Asp 50' is controlled by the binding of ADP: (1) The binding of ADP induces the movement of Asp 50' to stabilize Arg 339 (Fig. 3) to enhance the "side-to-side" intersubunit contact. Arg 339 interacts with the phosphorylated reaction intermediates. (2) The ADP binding also induces Asp 50' to move toward the ammonium binding site to enhance the ammonium binding, and then to deprotonate the ammonium ion to form the active ammonia to attack the  $\gamma$ -glutamyl phosphate (Alibhai & Villafranca, 1994).

### *Functions of Glu 327*

On the basis of the structure of the GS-MetSox complex (Liaw & Eisenberg, 1994), the ammonium ion site was proposed to lie near the methyl group of MetSox and near Glu 327, Glu 212, Tyr 179, and Asp 50', which were expected to participate in ammonium binding. However, the segment of GS around Glu 327 is not ordered in the presence of Tl<sup>+</sup> and ADP, suggesting that Glu 327 is not involved in ammonium ion binding. Residues 324–328 are stabilized only by MetSox, a transition-state analogue, and by no other effector of the 30 GS-effector complexes we have studied. This suggests that the glutamate binding flap, residues 324–328, may be stabilized only in the presence of the tetrahedral transition-state intermediate, perhaps by forming a salt link from Glu 327 to the positively charged  $\gamma$ -amino group of the intermediate. Therefore, we conclude that the function of Glu 327 is to stabilize the transition-state intermediate and to accept a proton from the  $\gamma$ -amino group of the intermediate to yield glutamine.

### *Extended structural model for glutamine synthesis catalyzed by GS*

On the basis of the X-ray structures presented here, we expand our earlier model for structure-based glutamine synthesis catalyzed by GS (Fig. 5 and Kinemage 2; our detailed schematic structural model, including the essential amino acid residues, is shown in Figure 4 of Liaw & Eisenberg [1994]). This structure-based model also rests on much earlier biochemical work from other laboratories, as summarized by Liaw and Eisenberg (1994), including the kinetic studies of Colanduoni et al. (1987). The two steps of the reaction are as follows: (1) ATP binds first at the top of the funnel-shaped active site cavity. The movement of Arg 359 toward the glutamate site, induced by ATP binding, enhances glutamate binding. Then glutamate binds at the bottom of the active site near a flexible loop, residues 324–328 (Fig. 5A and Kinemage 2). The  $\gamma$ -carboxylate group of glutamate attacks the  $\gamma$ -phosphate of ATP to produce  $\gamma$ -glutamyl phosphate and ADP. The presence of ADP induces movements of three residues: Arg 359 and Arg 339 interact with the  $\gamma$ -glutamyl phosphate, and Asp 50' moves toward the ammonium site (Fig. 5B and Kinemage 2). (2) The third substrate, ammonium, binds to its now fully formed binding site. Ammonium is deprotonated by Asp 50', permitting the resulting active ammonia to attack the  $\gamma$ -glutamyl phosphate, forming a tetrahedral intermediate. This tetrahedral intermediate stabilizes the glutamate binding flap, residues 324–328, because of interaction of its  $\gamma$ -amino group with Glu 327, covering the path of glutamate entry (Fig. 5C and Kinemage 2). Phosphate leaves and Glu 327 ac-

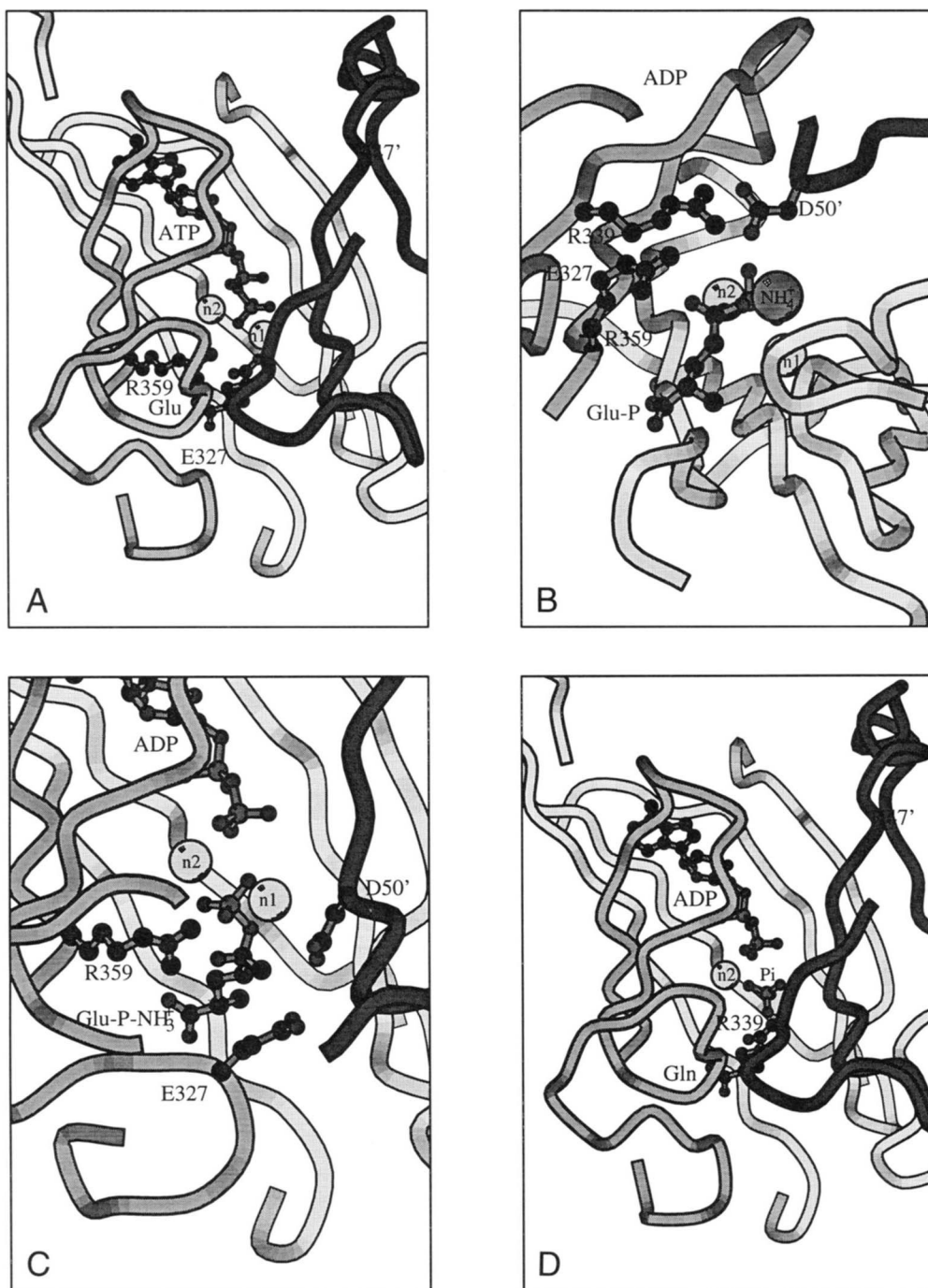


**Fig. 5.** An expanded structural model for the mechanism of glutamine synthesis catalyzed by GS, drawn by the program MOLSCRIPT (Kraulis, 1991). A full schematic structural model for the reaction, including the essential amino acid residues, was given in Figure 4 of Liaw and Eisenberg (1994). In A, C, and D, the active site is viewed from outside the GS dodecamer with the noncrystallographic sixfold axis vertical. The funnel-shaped active site is formed by two "side-by-side" adjacent subunits. Residues of the adjacent subunit, including Lys 47' or Asp 50', belong to the darker fragment. Panel A shows that ATP binds at the top of the active site and induces the movement of Arg 359 to increase the binding affinity of the second substrate glutamate, shown below metal ions  $n_1$  and  $n_2$ . The  $\gamma$ -carboxylate group of glutamate attacks the  $\gamma$ -phosphate of ATP to produce  $\gamma$ -glutamyl phosphate and ADP. Panels B and C show the progressing reaction at the glutamate pocket. In panel B, the molecule is rotated slightly to give the least obscured views of the important atoms, and in panel C, residues 338–340 are removed. Panel B shows that the presence of ADP induces the movement of Asp 50' to stabilize the interaction of Arg 339 with the  $\gamma$ -glutamyl phosphate, and to complete the ammonium ion site. It is here that the third substrate ammonia binds, and then is deprotonated by Asp 50' to form the more active ammonia. Panel C shows that ammonia attacks the  $\gamma$ -glutamyl phosphate to yield a tetrahedral intermediate,  $^+\text{NH}_3\text{-Glu-P}$ . The tetrahedral intermediate stabilizes residues 324–328 through the interactions of its  $\text{NH}_3^+$  group with Glu 327. Phosphate leaves and Glu 327 accepts a proton from the tetrahedral intermediate to yield the products glutamine (Gln) and phosphate (Pi), as shown in panel D.

**Table 2.** Summary of X-ray diffraction data for complexes of glutamine synthetase with monovalent cations

Crystal	Resolution (Å)	Unique/total reflections	Complete	$R_{\text{sym}}^a$	$\langle \Delta F \rangle / \langle F \rangle^b$
GS-Tl <sup>+</sup>	2.8	58,661/73,834	39%	7.8%	14.4%
GS-Tl <sup>+</sup> -ADP	2.8	87,370/126,467	58%	6.3%	14.1%
GS-Tl <sup>+</sup> -NH <sub>4</sub> <sup>+</sup>	3.0	51,436/64,112	42%	9.0%	14.2%
GS-Cs <sup>+</sup>	3.0	65,123/78,536	53%	11.4%	14.8%

<sup>a</sup> On intensity. A measure of the precision of data collection.

<sup>b</sup> Mean fractional isomorphous difference:

$$\frac{\sum \|F_{PH} - |F_P|\|}{\sum |F_P|}$$

cepts one proton from the  $\gamma$ -amino group of the intermediate to yield glutamine (Fig. 5D and Kinemage 2). The absence of biosynthetic activity of fully unadenylylated GS-Mn (Ginsburg & Stadtman, 1973) may be due to the strong interactions of the products ADP, Pi, and glutamine with the fully unadenylylated GS-Mn (Liaw & Eisenberg, 1994).

## Materials and methods

### Enzyme activity assay

The transferase assay was described originally by Levintow and Meister (1954). For the transferase assay, 250  $\mu$ L of reaction mixture, 100 mM triethanolamine, 50 mM dimethylglutarate, 10 mM KAsO<sub>4</sub>, 20 mM L-glutamine, 0.4 mM NaADP, 0.4 mM MnCl<sub>4</sub>, and variable concentrations of inhibitors and hydroxylamine, pH 7.0, are combined with 100  $\mu$ L of GS (1.5  $\mu$ g/mL) at 37 °C to start the reaction. After 10 min, the reaction is stopped by adding 1 mL of 3.3% FeCl<sub>3</sub>, 2% trichloroacetic acid, and 0.25 N HCl. The optical density at 540 nm is read on a Beckman DU-640 spectrophotometer 10 min later to determine the amount of glutamylhydroxamate produced.

### Crystal soaking and data collection

Fully unadenylylated GS from *S. typhimurium* was isolated by ammonium sulfate precipitation and a Cibracon blue affinity column in the presence of Mn<sup>2+</sup> (Liaw et al., 1993b). GS crystals were grown by the hanging drop method of vapor diffusion (Liaw et al., 1993a). Thallium acetate (with or without ADP) or CsCl was dissolved in the synthetic mother liquor and added to crystal-containing drops (Liaw et al., 1993b). Thallium acetate was saturated, and the estimated final concentrations of CsCl and Na·ADP were 30 mM and 1.6 mM, respectively. X-ray data from these GS-monovalent cation complexes were collected with an RAXIS-II (Rigaku) image plate detector (Table 2) at room temperature. All of these complex crystals were isomorphous with respect to native GS crystals, having space group C2 and unit cell dimensions  $a = 235.5$  Å,  $b = 134.5$  Å,  $c = 200.1$  Å, and  $\beta = 102.8^\circ$ .

### Fourier difference maps and refinement

Fourier difference maps, 12-fold averaged, using Fourier coefficients ( $F_{oGS-metal} - F_{oGS}$ ), were calculated by using CCP4 pro-

grams (SERC Daresbury Laboratory, 1994) implemented on a DEC VAX 4000 at UCLA. The initial phases of the 2.8-Å native GS model were used as phases of the complexes, as justified by the crystal isomorphism. Refinement of the atomic model to the X-ray data was performed using the program XPLOR 3.1 (Brünger et al., 1990). The final  $R$ -factor for the GS-Tl<sup>+</sup>-ADP complex is 23%, with RMS deviations for bond lengths being 0.12 Å, and for bond angles being 3°.

## Acknowledgments

We thank the Taiwan National Science Council for grant NSC 83-0412b002078 (to S.-H.L.) and the National Institutes of Health for grant GM-31299 (to D.E.), and Drs. J.J. Villafranca, G. Pflügl, and R. Weiss for discussions.

## References

- Alibhai M, Villafranca JJ. 1994. Kinetic and mutagenic studies of the role of the active site residues Asp 50 and Glu 327 of *E. coli* glutamine synthetase. *Biochemistry* 33:682-686.
- Almasy RJ, Janson CA, Hamlin R, Xuong N, Eisenberg D. 1986. Novel subunit-subunit interactions in the structure of glutamine synthetase. *Nature (Lond)* 323:304-309.
- Brünger AT, Krukowski A, Erickson JW. 1990. Slow cooling protocols for crystallographic refinement by simulated annealing. *Acta Crystallogr A* 46:585-593.
- Colandruoni J, Nissan R, Villafranca JJ. 1987. Studies of the mechanism of glutamine synthetase utilizing pH-dependent behavior in catalysis and binding. *J Biol Chem* 262:3027-3043.
- Coleman JE. 1992. Structure and mechanism of alkaline phosphatase. *Annu Rev Biophys Biomol Struct* 21:441-483.
- Cooper AJL, Plum F. 1987. Biochemistry and physiology of brain ammonia. *Physiol Rev* 67:440-519.
- Derouiche A, Frotscher M. 1991. Astroglial processes around identified glutamatergic synapses contain glutamine synthetase: Evidence for transmitter degradation. *Brain Res* 552:346-350.
- Drenth J, Hol WG, Jansonius JN, Koekoek K. 1972. A comparison of the three-dimensional structure of subtilisin BPN' and subtilisin novo. *Cold Spring Harbor Symp Quant Biol* 36:107-116.
- Ginsburg A, Stadtman ER. 1973. Regulation of glutamine synthetase in *Escherichia coli*. In: Prusiner S, Stadtman ER, eds. *The enzymes of glutamine metabolism*. New York: Academic Press. pp 9-43.
- Gursky O, Li Y, Badger J, Caspar DL. 1992. Monovalent cation binding to cubic insulin crystals. *Biochem J* 61:604-611.
- Hamberge A, Chiang GH, Nylén ES, Schiff SW, Cotman CW. 1979. Glutamate as a CNS transmitter. I. Evaluation of glucose and glutamine as precursors for the synthesis of preferentially released glutamate. *Brain Res* 168:513-530.
- Hill KA, Castellino FJ. 1986. The stimulation by monovalent cations of the amidase activity of bovine des-1-41 light chain activated protein C. *J Biol Chem* 261:14991-14996.

- Hill KA, Steiner SA, Castellino FJ. 1987.  $^{205}\text{Tl}^+$  as a spectroscopic probe of the monovalent cation binding sites of bovine plasma activated protein C and des-1-41-light-activated protein C. *J Biol Chem* 262:7098-7104.
- Kraulis PJ. 1991. MOLSCRIPT: A program to produce both detailed and schematic plots of protein structures. *J Appl Crystallogr* 24:946-950.
- Levintow L, Meister A. 1954. Reversibility of the enzymatic synthesis of glutamine. *J Biol Chem* 209:265-280.
- Liaw S, Eisenberg D. 1994. Structural model for the reaction mechanism of glutamine synthetase, based on five crystal structures of enzyme-substrate complexes. *Biochemistry* 33:675-681.
- Liaw S, Jun G, Eisenberg D. 1993a. Extending the diffraction limit of protein crystals: The example of glutamine synthetase from *Salmonella typhimurium* in the presence of its cofactor ATP. *Protein Sci* 2:470-471.
- Liaw S, Jun G, Eisenberg D. 1994. Interactions of nucleotides with fully unadenylylated glutamine synthetase from *Salmonella typhimurium*. *Biochemistry* 33:11184-11188.
- Liaw S, Pan C, Eisenberg D. 1993b. Feedback inhibition of fully unadenylylated glutamine synthetase from *Salmonella typhimurium* by glycine, alanine, and serine. *Proc Natl Acad Sci USA* 90:4996-5000.
- Liaw S, Villafranca JJ, Eisenberg D. 1993c. A model for oxidative modification of glutamine synthetase, based on crystal structures of mutant H269N and the oxidized enzyme. *Biochemistry* 32:7889-8003.
- Markham GD. 1986. Characterization of the monovalent cation activator binding site of *S*-adenosylmethionine synthetase by  $^{205}\text{Tl}$  NMR of enzyme-bound  $\text{Tl}^+$ . *J Biol Chem* 261:1507-1509.
- Meek TD, Villafranca JJ. 1980. Kinetic mechanism of *Escherichia coli* glutamine synthetase. *Biochemistry* 19:5513-5519.
- Meister A. 1980. Catalytic mechanism of glutamine synthetase; Overview of glutamine metabolism. In: Palacios R, Mora J, eds. *Glutamine: Metabolism, enzymology, and regulation of glutamine metabolism*. New York: Academic Press. pp 1-40.
- Mifflin BJ, Lea PJ. 1980. Ammonia assimilation. In: Mifflin BJ, ed. *The biochemistry of plants, vol 5: Amino acids and derivatives*. New York: Academic Press. pp 169-202.
- Naslund PH, Hultin T. 1981. Selectivity of interaction of univalent cations with mammalian ribosomes studied by equilibrium dialysis in the presence of the  $\text{K}^+$  analogue,  $^{204}\text{Tl}^+$ . *J Inorg Biochem* 14:67-79.
- SERC Daresbury Laboratory. 1994. *Collaborative computational project, number 4. The CCP4 suite: Programs for protein crystallography*. Warrington, UK: SERC Daresbury Laboratory.
- Stadtman ER. 1973. A note on the significance of glutamine in intermediary metabolism. In: Prusiner S, Stadtman ER. *The enzymes of glutamine metabolism*. New York: Academic Press. pp 1-9.
- Stadtman ER, Ginsburg A. 1974. The glutamine synthetase of *Escherichia coli*: Structure and control. In: Boyer P, ed. *The enzymes, vol 10*. New York: Academic Press. pp 755-807.
- Stellwagen E, Thompson ST. 1979. Activation of *Thermus* phosphofructokinase by monovalent cations. *Biochem Biophys Acta* 569:6-12.
- Stroud RM, Kay LM, Dickerson RE. 1974. The structure of bovine trypsin: Electron density maps of the inhibited enzyme at 5 Å and at 2.7 Å resolution. *J Mol Biol* 83:185-208.
- Suelter CH, Snell EE. 1977. Monovalent cation activation of tryptophanase. *J Biol Chem* 252:1852-1857.
- Takada J, Hioki Y, Yano M, Fukushima Y. 1990. A novel hydrophobic amine, (Z)-5-methyl-2-[2-(1-naphthyl)ethenyl]-4-piperidinopyridine, as a probe of the  $\text{K}^+$  occlusion center of  $\text{Na}^+/\text{K}^+$ -ATPase. *Biochim Biophys Acta* 1037:373-379.
- Urban BM, Hladky SB, Haydon DA. 1980. Ion movements in gramicidin pores. An example of single-file transport. *Biochim Biophys Acta* 602:331-354.
- Urry DW, Prasad KU, Trapane TL. 1982. Location of monovalent cation binding sites in the gramicidin channel. *Proc Natl Acad Sci USA* 79:390-394.
- van Driessche W, Zeiske W. 1985.  $\text{Ca}^{2+}$ -sensitive, spontaneously fluctuating, cation channels in the apical membrane of the adult frog skin epithelium. *Pflugers Archiv Eur J Physiol* 405:250-259.
- Yamashita MM, Almasy RJ, Janson CA, Cascio D, Eisenberg D. 1989. Refined atomic model of glutamine synthetase at 3.5 Å resolution. *J Biol Chem* 264:17681-17690.
- Zeiske W, van Driessche W. 1983. The interaction of " $\text{K}^+$ -like" cations with the apical  $\text{K}^+$  channel in frog skin. *J Membrane Biol* 76:57-72.